Metal Transfer during GMAW with Thin Electrodes and Ar-CO_2 Shielding Gas Mixtures

Droplet diameters do not decrease proportionally with electrode diameters as small as 0.016 in. and repelled transfer mode is dominant above 30% CO_2

BY E. J. SODERSTROM AND P. F. MENDEZ

ABSTRACT. Metal transfer modes in gas metal arc welding (GMAW) using direct current electrode positive (DCEP) in a variety of binary Ar-CO_2 shielding gas mixtures and electrodes with diameters as small as 0.016 in. (0.41 mm) were investigated. Droplet detachment frequency was determined by analyzing the voltage signal with Fast Fourier Transform, and the results were verified with high-speed laser shadowgraph techniques. A newly designed contact tip was used with the thinnest electrode that improved process stability at feed rates up to 1443 in./min. It was found that the average droplet diameter in the spray region did not decrease proportionally with electrode diameters. When using small-diameter electrodes (<0.035 in.) with shielding gas mixtures containing less than 30% CO_2, the average droplet diameters did not become smaller than electrode diameters, regardless of the current used. Repelled transfer was dominant with shielding gas compositions containing more than 30% CO_2 regardless of electrode diameter.

Introduction

Gas metal arc welding (GMAW) is currently the most widely used arc welding process in industry. Benefits such as high production rates, high weld quality, ease of automation, and the ability to weld many metals make it attractive to manufacturers. One of the unique characteristics in this process is the way molten metal is transferred across the arc. The transfer of metal from the electrode to the workpiece influences penetration, bead morphology, fume generation, process stability, and spatter. Metal transfer is controlled by several parameters, including current, voltage, polarity, electrode extension, shielding gas composition, and electrode diameter.

The choice of shielding gas affects welding quality through its influence on metal transfer and also has a direct impact on welding costs. CO_2 is more plentiful, widely available, and less expensive than argon; however, weld bead quality and deposition rates often decrease with the increase of CO_2 in a binary Ar-CO_2 mixture. Currently, argon costs two to three times as much as CO_2. If it were possible to create welds of the same quality and deposition rates of high Ar mixtures with less expensive mixtures containing significant amounts of CO_2, the savings in the welding industry would be substantial.

This research studied the transition between globular and spray transfer in Ar-CO_2 atmospheres. What differentiates this work from previous investigations is that behavior of thin electrodes (as small as 0.016 in. diameter) is explored. The motivation to study these thin electrodes is the possibility that they might avoid globular and repelled transfer, as is discussed later. Our experiments show that this is not the case with DCEP welding, but that an unexpected metal transfer mechanism occured. To the best of the authors' knowledge, there is no published research on metal transfer with electrodes smaller than 0.030 in. (0.76 mm).

KEYWORDS

Gas Metal Arc Welding
Droplet Detachment
DCEP
CO_2 Shielding Gas
Contact Tip
Metal Transfer Modes

*E. J. SODERSTROM (*esoderst@mines.edu*) is a graduate student and P. F. MENDEZ (*pmendez@mines.edu*) is assistant professor, Colorado School of Mines, Golden, Colo.*

Previous Research on Metal Transfer

The American Welding Society (AWS) and the International Institute of Welding (IIW) have classified metal transfer into different categories (Refs. 1, 2). For GMAW applications, the two main categories are short circuiting and free flight. Short circuiting transfer is characterized by the electrode periodically contacting the weld pool. The electrode never contacts the weld pool during free-flight transfer; molten droplets detach from the electrode, travel through the arc, and are deposited on the base metal. Free-flight transfer is usually divided into subcategories that include globular, spray, rotating, and repelled (nonaxial globular). Observations of metal transfer during GMAW began to be published in the 1950s and continue to be of interest in research because of its direct application to industrial conditions.

A key aspect of free-flight metal transfer in GMAW is the existence of a relatively sharp "transition current." Among the first to report on this transition current were Muller, Greene, and Rothschild (Ref. 3). They used DCEP polarity and showed that metal transfer is influenced by the type of shielding gas, the electrode composition, welding current, voltage, and electrode extension.

Below the transition current, metal is transferred in the form of large droplets (globular transfer). In this regime, the diameter of the droplets is often larger than the wire diameter, and the frequency of droplets is relatively low. Above the transition current, metal is transferred as small droplets at a relatively high frequency (spray transfer).

For example, Lesnewich (Refs. 4, 5) reported a transfer rate of 5 Hz for droplets of 0.16 in. diameter in the globular regime with 0.0625-in.- (1.59-mm-) diameter electrode, argon+1%O_2 shielding. In the spray transfer regime, he reported a de-

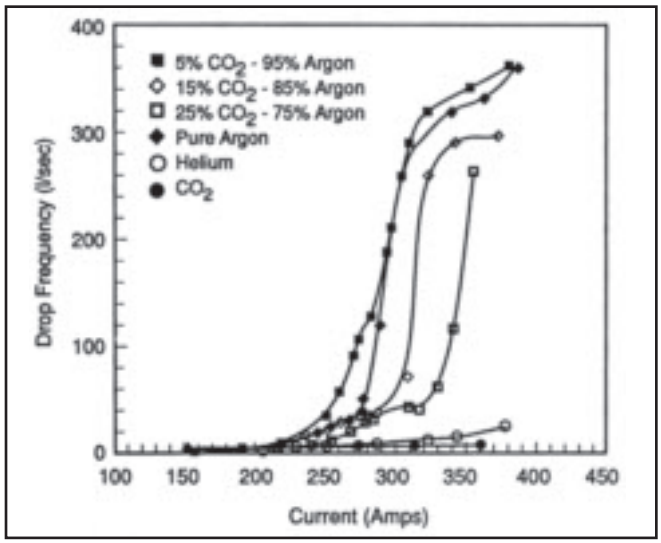

Fig. 1 — Effect of shielding gas composition on transition region using 0.0625-in.- (1.59-mm-) diameter electrodes. Increasing amounts of CO_2 increase transition currents until the transition from globular to spray is replaced by the occurrence of repelled transfer (Ref. 11).

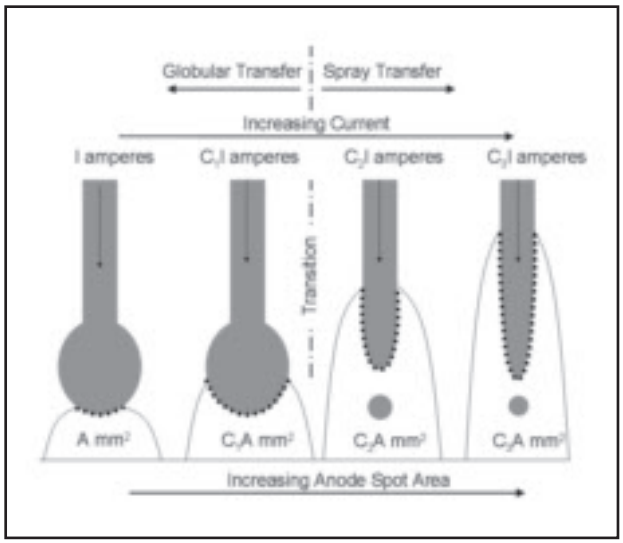

Fig. 2 — Schematic showing the effects of increased welding current in argon. The current density at the anode spot (dotted lines) remains constant. When current increases, the anode spot area increases. $1<C_1<C_2<C_3$. Transfer mode changes when the anode spot envelops the droplet.

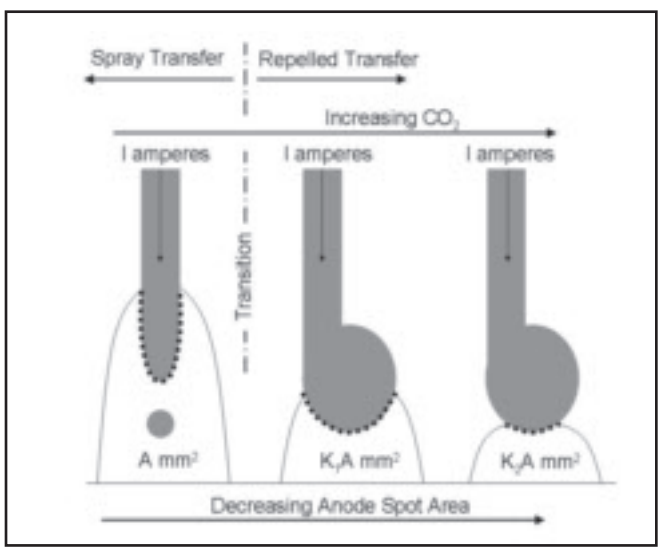

Fig. 3 — Schematic showing the effects of CO_2 on current density and metal transfer. $1>K_1>K_2$. The current density becomes higher with increasing amounts of CO_2, resulting in a smaller anode spot at the same current, and changing the transfer mode from spray to repelled.

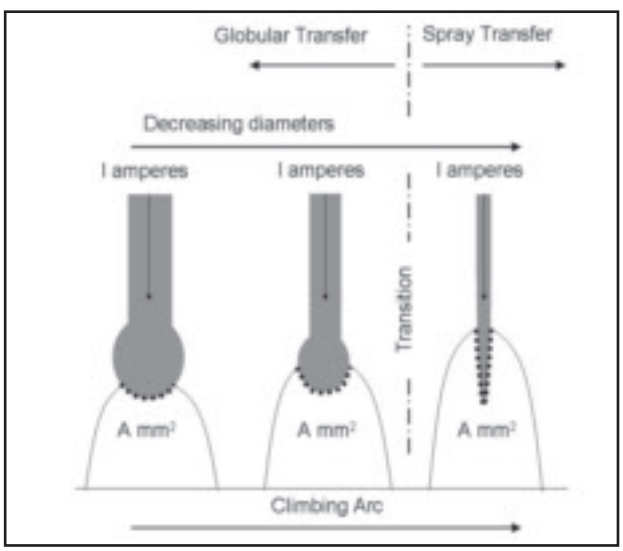

Fig. 4 — Schematic drawing showing the effects of decreasing electrode diameter. The current density remains constant, but a change in transfer mode occurs due to position of the arc attachment point.

tachment frequency of 240 Hz for droplets of 0.04 in. diameter. The maximum measured current for pure globular transfer was 255 A, and the minimum measured current for pure spray transfer was 265 A. Lesnewich defined the transition current as the average between these limiting values (260 A in this case). In this work, we use the same definition.

The exact mechanism that causes the transition in metal transfer mode is not yet fully understood; however, two main theories have provided good results in the analysis of metal transfer: pinch instability theory (PIT) and static force balance theory (SFBT). Rhee and Kannatey-Asibu (Ref. 6) analyzed both and found that SFBT gives good predictions for the globular regime, and PIT is better for the spray regime. During the transition from globular to spray, neither theory by itself is accurate in predicting metal transfer. Recently, computer models have enabled a better understanding of the physics of metal transfer. A GMAW simulation model based on computational fluid dynamics generated predictions of droplet diameters that agreed well with experimental values in the transition region (Ref. 7). A comprehensive model for metal transfer in GMAW was developed by Hu and Tsai (Ref. 8); with it, they were able to predict droplet size, detachment, and velocity for both constant and pulsed current conditions.

Previous Research on Carbon Dioxide in Shielding Gas

Cost savings were identified as early as 1956 when Rothschild (Ref. 9) reported that CO_2 shielded arc welding was a feasi-

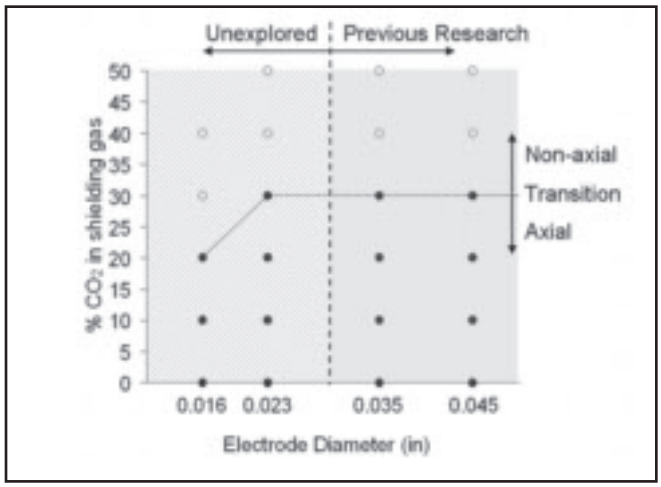

Fig. 5 — Experimental matrix used in this research. Solid circles represent full data collection parameters and hollow circles represent exploratory experiments. The transition line marks the area of mixed transfer, where both nonaxial and axial detachments are observed.

ble alternative to argon during the joining of mild steel. Using uncoated steel electrodes and nonpulsed power supplies with DCEP, Smith (Ref. 10) reported stable, axial types of free-flight transfer when the CO_2 concentrations are less than 25%. Above 25% CO_2, the operating characteristics of the process changed to repelled transfer during free-flight mode; however, using short circuiting transfer, quality welds could be made with 100% CO_2 at decreased deposition rates.

The addition of CO_2 in the shielding gas increases the transition current and decreases the maximum droplet detachment frequency, as shown in Fig. 1. Researchers (Ref. 11) conducted experiments using varying compositions of shielding gas with 0.0625-in. (1.59-mm) steel electrodes. These changes are apparent up to 25% CO_2, then the process exhibits repelled transfer as the dominant mode of metal transfer at all currents.

Higher amounts of CO_2 in the shielding gas leads to constriction of the arc, which results in repelled transfer. Haidar and Lowke reported an increase in anode spot current density from 7×10^3 to 3.3×10^4 A/cm^2 as CO_2 concentration increases from 0 to 100% (Ref. 12). Mechev et al. (Ref. 13) showed through calculations that the CO_2 arcs are more constricted; the dynamic processes that occur in a CO_2 arc are concentrated within a narrower region when compared to argon. The interactions between the plasma and the electrode, including chemical reactions, spatter formation, and droplet detachment are significantly changed with additions of CO_2. Nemchinsky (Ref. 14) developed a model for current conduction in the near-anode plasma layer and compared current distributions between argon, helium, and molecular gases. The results agree with observations that arc constriction and current distribution over the anode surface is controlled by the plasma gas. Pires et al. (Ref. 15) recently proposed a similar model involving arc envelopment and anode spot contraction that was supported with experiments using seven different Ar-O_2-CO_2 gas mixtures.

Two approaches to improve free-flight metal transfer with CO_2 levels above 25% have been proposed. The first approach uses an electrode with dilute coatings, and the second approach uses pulsing power supplies. Dilute coatings of alkali and rare earth metals on the electrode were investigated at Airco by Lesnewich (Ref. 16) and Cushman (Ref. 17). They developed an electrode that operated in 100% CO_2 shielding gas that gave stable metal transfer and generated much less spatter than uncoated electrodes. The researchers concluded that spray transfer is impossible when the path of welding current at the tip of the electrode is confined to a small high-current-density area, and postulated that by having negative polarity on the electrode and adding thermionic emissive agents to the surface of the electrode, they could control the current density at the tip of the electrode.

The second approach uses pulsing of the welding current or voltage. Controlling the current is one of the main advantages of pulsed power supplies because it directly affects the EM forces and metal transfer mode. Needham and Carter (Ref. 18) showed it is possible to have better quality welds made at larger deposition rates in CO_2 when using pulsed current. Nonetheless, this new technology was unable to surpass the deposition rates and cleanliness of welds made with argon-based shielding gases. Later, Matsuda et al. (Ref. 19) used an adjustable rectangular-wave pulse machine to create welds in CO_2. Using a 0.045-in.- (1.14-mm-) diameter electrode, mean current of 250 A, and pulsing frequencies of 38 Hz, welds were made in CO_2. This reduced the spatter to 20% of the nonpulsed process.

Current state-of-the-art processes for GMAW with CO_2 do not use free-flight transfer; instead, they use advanced short circuiting metal transfer. Sophisticated computer program control of welding parameters enables waveforms never before used in GMAW. In this technology, the droplet is formed with a large current pulse, dipped into the weld pool, and detached by surface tension. Power source manufacturers offer several variations on this technology, which modulates the power input very quickly in order to reduce the amount of spatter. Miller Electric's Regulated Metal Deposition (RMD™) and Lincoln Electric's Surface Tension Transfer (STT®) are two variations of this technology available for use in industry. Deposition rates are approaching those of free-flight transfer, but limiting factors such as stubbing and arc length changes become prominent at high wire feed speeds. Recent developments combine the use of pulsing and high-speed reversible wire feeding to address these issues, as described by Cuiuri et al. (Ref. 20).

Table 1 — Electrode Diameters and Compositions Used in This Research

Wire Diameter (in.)	AWS Classification	Composition (wt-%)					
		C	Mn	Si	P	S	Cu
0.045	ER70S-6	0.07	1.40	0.80			
0.035	ER70S-6	to	to	to	0.025	0.035	0.50
0.023	ER70S-6	0.15	1.85	1.15			
0.016	ER70S-G	0.13	0.51	0.08	0.010	0.010	0.62

Behavior of Anode Spot

The envelopment of the droplet by the arc is essential to the metal transfer mode, therefore it is useful to analyze it in detail. Through experimental observation, Rhee and Kannatey-Asibu (Refs. 6, 11) reported that the globular/spray transition occurs when the arc covers the droplet surface and suggested that helium and CO_2 shielding gases do not exhibit transition because the arc does not climb over the droplet. This evidence suggests that the transition from globular to spray occurs when the arc covers the entire droplet. Arc envelopment of the droplet is expected to change the distribution of forces upon the droplet, thus directly influencing the transfer mode.

The mechanism of envelopment of the droplet in an argon rich atmosphere is illustrated schematically in Fig. 2. In this

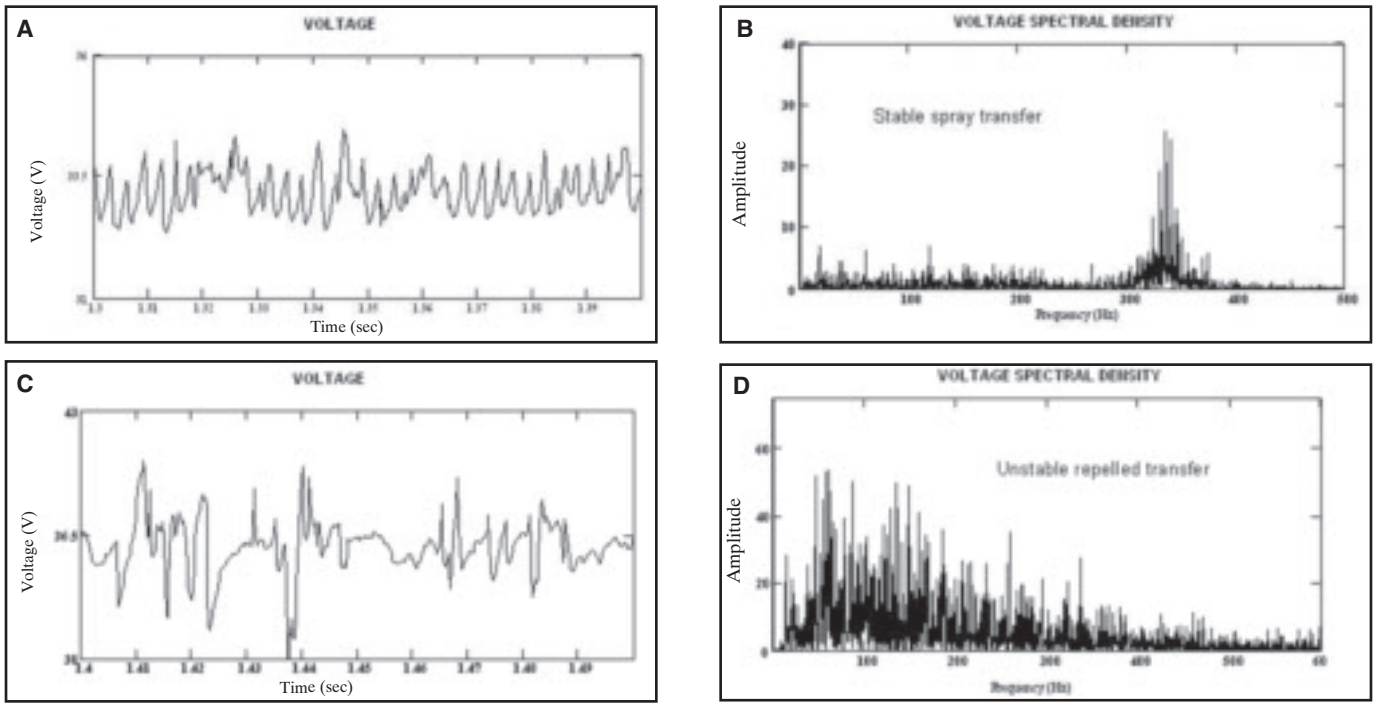

Fig. 6 — A — Voltage signal of a weld made with 0.035-in.-diameter electrode in a 90Ar-10CO_2 shielding gas mixture; B — Fast Fourier Transform (FFT) of A. The voltage signal is fairly periodic, leading to a distinguishing frequency peak in the FFT. C — Voltage signal of a weld made with 0.035-in.-diameter electrode in 60Ar-40CO_2 that shows repelled metal transfer. Droplet detachment is random and nonaxial; D — FFT of C.

case, the current density at the anode spot is approximately constant, independent of current or droplet size (Ref. 12). At low currents, represented on the left side, the anode spot covers only a small portion of the droplet's surface area, A. In the figure, the anode spot area is represented by the dotted interface. Globular transfer is the dominant transfer mode, having droplet diameters larger than the electrode. As the current increases from I to C_1I, the anode spot area increases to C_1A as well, but does not completely envelop the droplet. Transition occurs at higher currents, when the current increases to C_2I, and the relative anode spot area, C_2A, becomes large enough to cover the entire droplet. At this point, the arc attachment is above the droplet and climbing up the electrode, climbing even higher as current increases to C_3I. At these high currents, more of the electrode is in the arc and melting occurs radially, creating a taper. The morphology of the taper and relative size of the droplets will determine whether the spray transfer is projected or streaming spray. In projected spray transfer, the electrode has a short taper with droplets slightly smaller than the diameter of the electrode. Streaming spray has an electrode with a long taper and the droplets are much smaller than the electrode.

Shielding gas composition can change the metal transfer mode with all other variables held constant. Experimental observations of arc constriction indicate that current density depends mainly on shielding gas composition. Figure 3 is a schematic that illustrates how increasing amounts of CO_2 in the shielding gas alters the metal transfer mode. From left to right, the CO_2 concentration is increasing in the shielding gas. When concentrations approach a critical level, a transition occurs where metal transfer changes from axial spray to repelled transfer. Greater amounts of CO_2 increase the current density at the electrode. For a constant current, the anode spot becomes smaller with increasing amounts of CO_2. If the anode spot becomes small enough that it is unable to cover the droplet, the transfer mode changes from spray to globular. Depending on the current and current density values, the plasma pressure concentrated in a small area on the droplet can result in a force large enough to levitate the droplet, resulting in repelled transfer. The increase in anode spot density with CO_2 is not well known, and it is not necessarily linear.

For typical electrode diameters, their size also influences the metal transfer mode. Figure 4 shows the effects that diameter has on the transition from globular to spray transfer. At a given current and shielding gas composition, the arc attachment point is located under the droplet for the largest electrode. As the diameter of the electrode is decreased, the arc attachment point climbs up the droplet because current density remains the same. When the electrode diameter becomes small enough, the arc attachment point moves above the droplet and results in a transition from globular to spray.

Because the current density at the electrode tip is a function of shielding gas, increasing the amount of CO_2 will increase the current density, such that the anode spot area will decrease for a given current and lead to arc constriction on the droplet. This work explores whether this effect could be counteracted by decreasing electrode diameter such that the arc attachment is forced above the droplet, enveloping it, and causing a transition to spray transfer.

Procedure

Experimental Matrix

Figure 5 shows the experimental matrix followed in this research. The circles shown on the graph represent particular welding parameters used. The full circles are the focus of this research, while the hollow circles represent parameters where repelled transfer occurred and prevented further measurements. The dotted line shows the transition region where the transfer was mixed between nonaxial (repelled) and axial types of detachments. On the graph, the double cross-hatched shad-

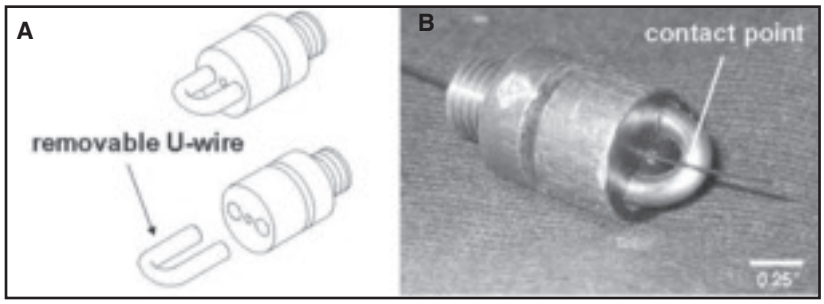

Fig. 7 — Schematic of the newly designed contact tip (A) and the fabricated part (B). The electrical contact point is restricted to the point shown. An insulating alumina tube lines the hole in the main body.

ing on the right shows regions where published data were found. On the left, the single cross-hatched region shows unexplored parameters for electrode diameters and shielding gas compositions. From the conditions that are shown on the graph, testing revealed that repelled transfer begins to dominate when concentrations of CO_2 are at or above 30% for electrode diameters 0.023 in. (0.58 mm) and larger. For the 0.016-in.- (0.41-mm-) diameter electrode, repelled transfer becomes dominant at 20% CO_2.

For a given electrode diameter and shielding gas composition, the transition current was determined using Lesnewich's definition described previously. The tests began at low wire feed speeds (WFS) that corresponded to globular transfer mode and relatively low currents. The WFS was increased until a transition was observed and spray transfer mode becomes dominant. Voltages were adjusted in order to keep the electrode extension constant. Contact tip-to-workpiece distance (CTWD) remained constant for each electrode diameter tested. The three largest electrodes were tested with 1.0-in. (25.4-mm) CTWD and 0.5-in. (12.7-mm) arc length. The 0.016-in.- (0.41-mm-) diameter electrode was tested using 0.75-in. (19.1-mm) CTWD and 0.38-in. (9.7-mm) arc length for improved process stability.

Droplet Diameter Measurement

Comparing droplet size to wire diameter is useful, since the traditional criterion of globular transfer is stated in those terms. For the parameters tested, high-speed laser shadowgraphs indicated that the detaching droplets have a shape close to spherical for nonrepelled transfer. Droplet diameters can be calculated using a volume balance resulting in the following expression:

$$d_d = \left(\frac{WFS \cdot d_e^2}{40 \cdot f_d} \right)^{\frac{1}{3}}$$

where d_d is the droplet diameter in inches, *WFS* is the wire feed speed in inches/minute, d_e is electrode diameter in inches, and f_d is the droplet detachment frequency in Hertz. This calculation assumes that losses due to evaporation are small, and requires a measurement of the droplet detachment frequency.

Frequency Measurement

In this work, two methods were used to measure droplet detachment frequency: Fast Fourier Transform (FFT) of the voltage signal, and high-speed laser shadowgraph. FFT of the current signal was also performed, but was of inferior quality than the FFT from voltage.

Fast Fourier Transform (FFT) is simple to implement and accurate for the stable transfer cases, in which a peak in the FFT spectrum is clearly discernible. In our case, the FFT spectra were generated by sampling the voltage signals at 5 kHz for 5 s. Figure 6 shows the voltage waveforms and the FFT plots for both stable and repelled metal transfer. During stable metal transfer, the voltage waveform shows a relatively stable frequency and amplitude. The sharp peak in a narrow frequency range in Fig. 6B indicates that detachment frequency is relatively constant, and constrained within a narrow range. In this case, the peak in frequency distribution begins at approximately 300 Hz, has a maximum value at 340 Hz, and ends at approximately 375 Hz. This spread in frequencies corresponds to a spread in droplet diameter between 0.037 and 0.039 in. (an error of approximately 5%).

When the transfer mode approaches repelled transfer, droplet detachment becomes erratic and the FFT spectrum becomes broad, without a clearly identifiable peak representative of the detachment frequency. The distinctly different waveform and FFT are shown in Fig. 6D. The broad spectra distributed over a large frequency range represent the inconsistent timing of detachment events.

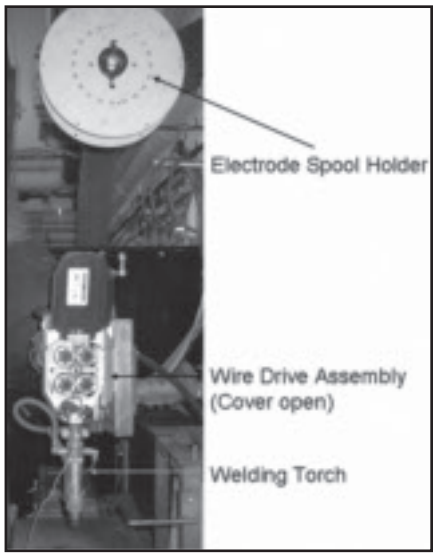

Fig. 8 — A detailed view of the modified wire feeding unit. The distance from the end drive rolls to the welding gun has been minimized to prevent buckling and allow smooth feeding of small-diameter electrodes.

Droplet detachment frequency was also measured using high-speed laser shadowgraphs. In this case, images were taken at 3000 frames per s., and detachments were counted for three separate 0.1-s intervals of the run. Because of its simplicity of use, most of the frequencies reported in this work correspond to the peak frequency of the FFT spectrum. When the FFT spectrum did not show a sharp peak, the frequency reported corresponds to the droplet counting technique using high-speed video. The agreement between the two frequency measurement techniques was tested for stable globular/spray transfer modes. In this case, both measurements are within 10% of each other for all electrode diameters, consistent with previous observations by other researchers (Refs. 21–23).

Materials

Flat position bead-on-plate welds were made on 0.375-in.- (9.5-mm-) thick ASTM A36 bars using four different electrode diameters ranging from 0.045 to 0.016 in. (1.14–0.41 mm). Table 1 gives the chemical compositions of the different electrodes. The three largest electrodes were commercially available ER70S-6 welding electrodes manufactured by Hobart. Smaller electrode diameters are not commercially available, so a special 0.016-in.-diameter electrode was manufactured by California Fine Wire Co. Industrial-grade argon and CO_2 were used as shielding gases. Mixtures of 100Ar, 90Ar-10CO_2, 80Ar-20CO_2, and 70Ar-30CO_2 were used for the four different electrode sizes.

No commercially produced contact tubes were available for the 0.016-in.-diameter electrode, so two different types were fabricated. The first design followed the conventional tube-type contact tip configuration. Meltback events increased as electrode diameters became smaller because of the sensitivity of the system. Small changes in current have larger effects on electrode extension with smaller electrodes. Also, the point of electrical contact is unknown due to the variability of contact points within the tube. Waszink and Van Den Heuvel have estimated this point to shift as much as 0.050 in. (1.25 mm) during the welding operation (Ref. 24). As the electrical contact points vary, so does the effective electrode extension. A new design was needed as electrode diameters became smaller and process stability became more sensitive to small changes in welding parameters.

Figure 7 shows the new design for the contact tip used with the 0.016-in.-diameter electrode. The function of the device relies on the stiffness of the electrode to establish electrical contact with the tip. The point at which the electrode intersects the U-wire is the exact place of electrical transfer and was used to measure the CTWD. This ensures that the electrode extension is kept constant, unlike traditional tube-style contact tips. This feature reduces the amount of meltbacks when compared to the conventional design and enables a fast change when they do occur. This new design is well suited for thin electrodes (0.016 in.) because it avoids the tight manufacturing tolerances of the small hole of a conventional contact tip. The improved performance of this new contact tip suggests that process stability can be improved by precisely controlling the point of electrical contact between the electrode and the contact tip. A patent is pending for the design of the new contact tip (Ref. 25).

Equipment

The power source used in this research was a Miller Electric Maxtron 450 CC/CV power supply operated in CV mode. No pulsing or waveform programming was implemented in the experiments. The wire feed machine was a constant-speed Miller Electric S-70 with high-speed motor option, capable of feed rates up to 1443 in./min. Several modifications were made to the unit to improve the performance during this research, shown in Fig. 8. The distance between the contact tip and the drive rolls was minimized from 72 to 8 in. for better feeding of thin electrodes. An adapter was fabricated that repositioned the welding gun immediately adjacent to the wire drive assembly.

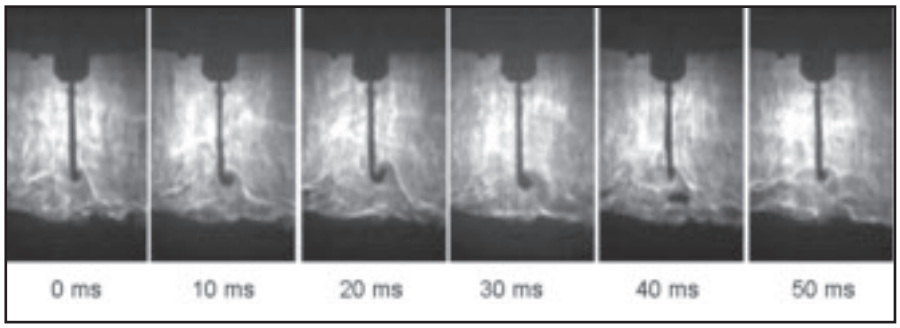

Fig. 9 — High-speed shadowgraphs of repelled transfer during welding using a 0.035-in. electrode in a 60Ar-40CO_2 shielding atmosphere. The contact tip shadow is clearly visible at the top of the screen, with the electrode shown in the middle. The droplet first moves upward before detaching from the electrode.

An Omega gas proportioning rotameter was used for varying the composition of the shielding gas. A calibrated flowchart was supplied from the manufacturer for the binary Ar-CO_2 gas mixtures. Constant flow rates of 40 ft^3/h were used throughout the entire study. The mixer was received from the factory calibrated with an accuracy of ±2% in composition.

In this work, laser shadowgraph techniques and a high-speed digital camera were used to image metal transfer. The system used in this research was similar to that of Allemand's (Ref. 26). The laser source was a helium-neon laser manufactured by Melles-Groit with a maximum output of 30 mW at a wavelength of 632.8 nm. The beam passed through a spatial filter, collimator, aiming mirror, and then the arc. On the other side of the arc, the beam traveled through a bandpass interference filter, allowing light in the range of 632.8 ± 0.5 nm to pass. The shadow of the contact tip, electrode, droplets, and base metal were projected onto a piece of frosted glass and filmed with high-speed video. A Kodak Ektapro EM digital high-speed camera was used to record the welding process. Figure 9 shows a compilation of screenshots taken from the same experiment as Fig. 6C, D. The frames are 10 ms apart, during repelled transfer using a 0.035-in. electrode in a 60Ar-40CO_2 shielding gas mixture.

The second method for determining metal transfer mode used voltage and current analysis. Both the current and voltage transducers were manufactured by LEM, with the signal conditioning units made in-house. A National Instruments data acquisition system interfaced to a computer, where National Instruments Labview program was used as the control software. The sensors were calibrated with a Fluke multimeter having both voltage and current measuring capabilities. For all experiments, the voltage and current signals were sampled at 5000 Hz for approximately 5 s, and then analyzed using MATLAB.

Results and Discussion

Welding Current Effects

Figures 10–13 show the relationship between average droplet diameter and welding current for the four electrode diameters tested with different shielding gas mixtures. Several distinguishable trends can be noted. Shielding gas composition seems to have little influence on droplet size for currents above the transition. Shielding gas compositions containing more than 30% CO_2 exhibited substantial amounts of repelled transfer and are not included in these plots for the 0.045-, 0.035-, and 0.023-in.-diameter electrodes. Shielding gas compositions only up to 20% CO_2 are shown in Fig. 13 because repelled transfer occurred above this gas composition. It is unclear whether this effect is due to the extremely small electrode diameter or to the small differences in chemical composition of that electrode.

Droplet Diameter

Figure 14 shows the relationship between average droplet diameter and current for the different diameter electrodes tested in a 90Ar-10CO_2 atmosphere. All electrodes exhibit a transition from large droplet diameters (low detachment frequency) to small droplet diameters (high detachment frequency). After the transition, a lower shelf for droplet diameters exists for all electrodes. For the 0.045-in. electrode, calculations indicate that the average droplet diameter becomes smaller than the electrode diameter. This observation is consistent with several other researchers, and has been the traditional definition of spray transfer.

The 0.035-, 0.023-, and 0.016-in.-diameter electrodes still exhibit the same type of transition from large to small droplet diameters with increasing current. Past the transition, the transfer mode would appear and sound like spray transfer to the

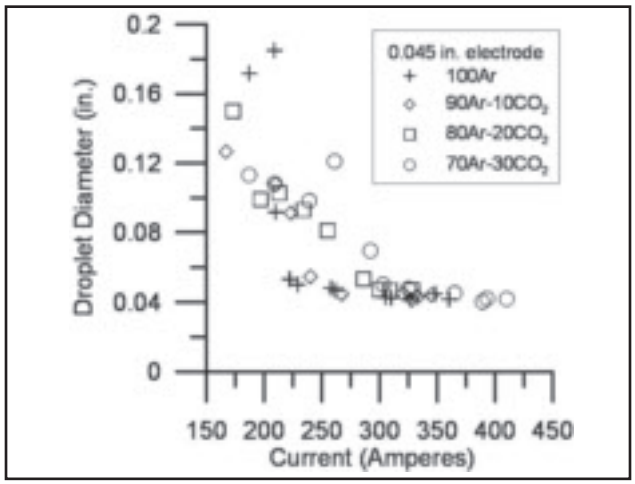

Fig. 10 — The average calculated detached droplet diameter as a function of current for the 0.045-in. electrode with different shielding gas compositions.

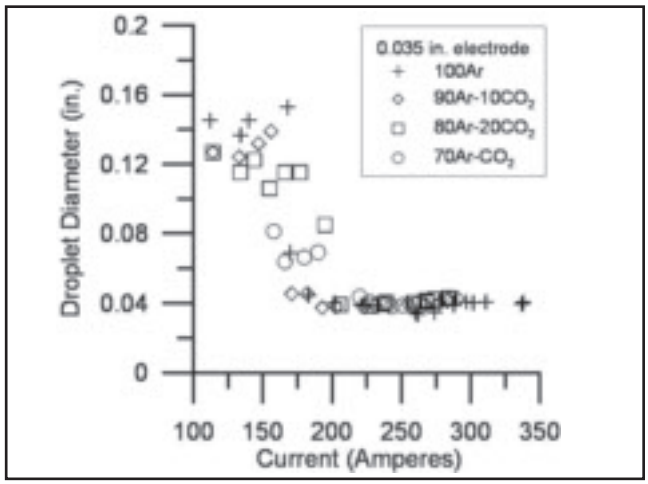

Fig. 11 — The average calculated detached droplet diameter as a function of current for the 0.035-in. electrode with different shielding gas compositions.

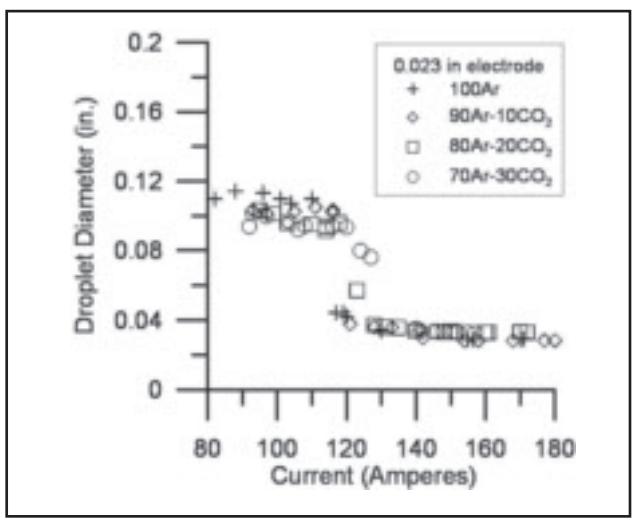

Fig. 12 — The average calculated detached droplet diameter as a function of current for the 0.023-in. electrode with different shielding gas compositions.

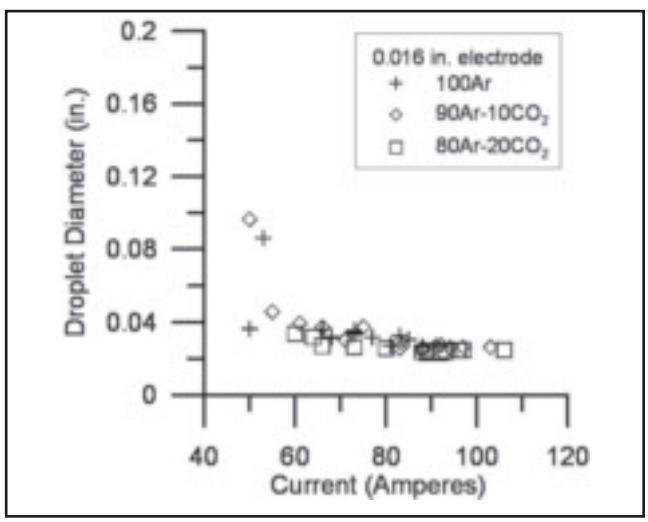

Fig. 13 — The average calculated detached droplet diameter as a function of current for the 0.016-in. electrode with different shielding gas compositions.

senses of a skilled welder; however, it would not fit to the traditional definition of spray transfer. Analysis shows that the average droplet diameters do not become smaller than the electrode diameters. The traditional spray definition that droplet diameters are smaller than electrode diameters is not applicable to small-diameter electrodes. Figure 14 shows the results for a 90Ar-10CO_2 shielding gas mixture, and the same trends are evident with the 100Ar and 80Ar-20CO_2 mixtures.

The change in minimum droplet diameter is smaller than the change in their associated electrode diameters. Figure 15 shows the average droplet size just after the transition as a function of electrode diameter for 90Ar-10CO_2 gas mixtures. As the electrode diameter changes from 0.045 to 0.035 in., the average droplet size only changed from 0.042 to 0.038 in. These small variations of spray transfer droplet diameter with wire diameter may be controlled by surface tension; however, initial calculations indicate that additional factors not yet identified must be at play.

Shielding Gas Effects

Free flight mode begins to become repelled with concentrations of CO_2 between 20 and 30%. This is consistent with several other researchers' observations and can now be extended to electrodes with diameters as small as 0.016 in. The addition of CO_2 does not have a proportional influence on metal transfer. In this research, there is little effect until CO_2 concentrations reach 30% and then repelled transfer begins to appear, as shown in Fig. 16. The transition current was determined using Lesnewich's definition described above. The smallest (0.016-in.-diameter) electrode is not included in this graph because an upper limit in the spray region was not found, since it occurs at wire feed speeds beyond the capability of the equipment.

A transition from large-diameter droplets to small-diameter droplets occurs for all-diameter electrodes in shielding gas concentrations of up to 30% CO_2 as the current is increased.

The effect of shielding gas on transition current is a relatively gradual increase for the 0.045-in. wire, while it shows a little effect, even a slight decrease, for the 0.023- and 0.035-in. wires. The behavior of the transition current for the largest electrode (0.045-in.) is consistent with that de-

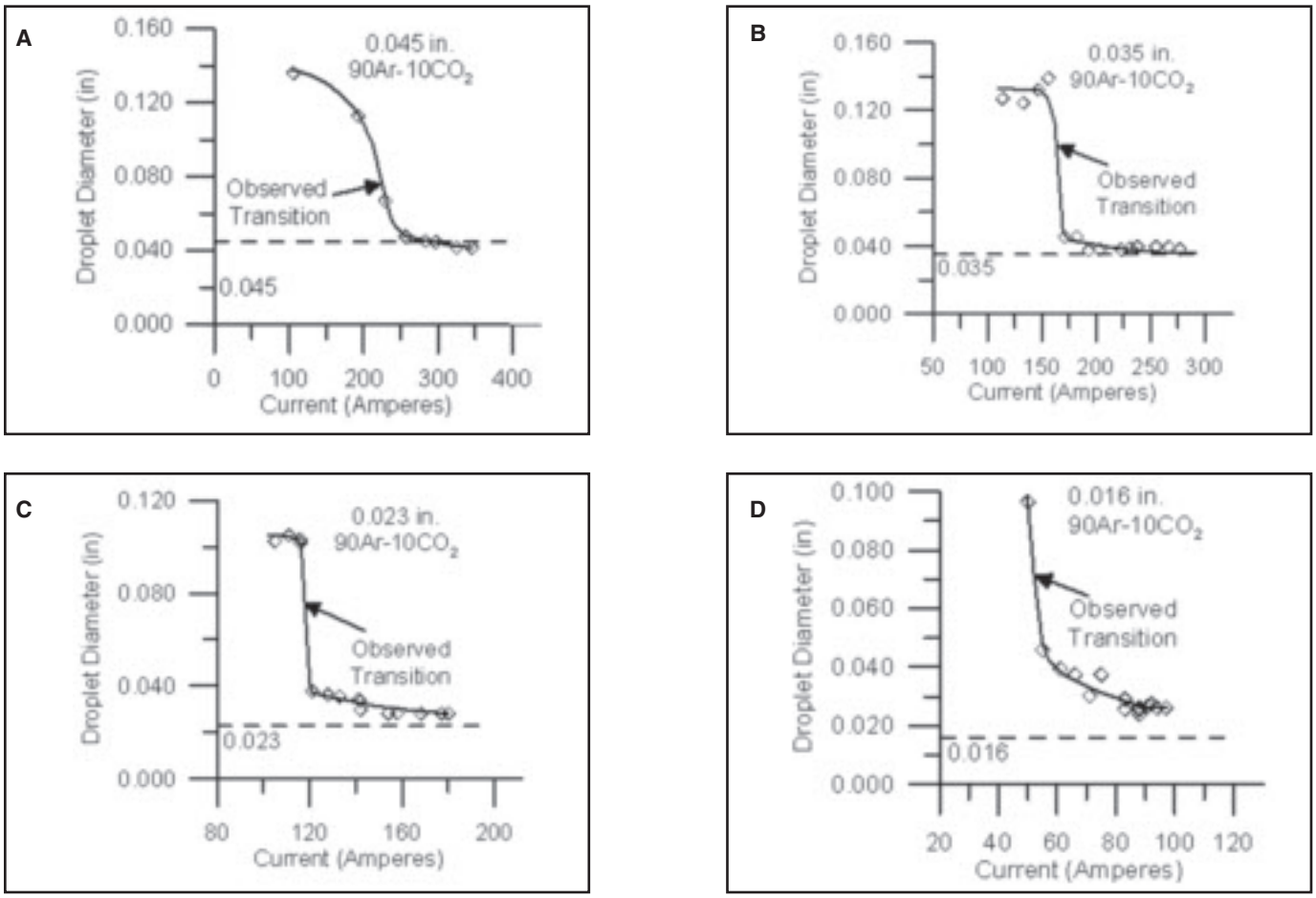

Fig. 14 — Characteristics between droplet diameter and current for four different electrode diameters. The droplet diameters never become smaller than electrode diameters in the three smallest electrodes.

scribed in the schematic of Fig. 3, in which a more constricted anode spot requires larger currents to envelop the droplet and create the transition. The effect of CO_2 on the thinner wires does not follow this pattern, suggesting that the behavior of the anode spot in thin electrodes involves factors that are not relevant for larger electrodes. This effect is currently being investigated.

At shielding gas concentrations of 80Ar-20CO_2, the dominant transfer is stable axial, whether within the globular or spray regime. For shielding gas mixtures containing 60Ar-40CO_2, repelled transfer becomes dominant at all currents. The mixture at 70Ar-30CO_2 shows a mixed mode. At this level, repelled transfer begins to become apparent not only through high-speed video but also through increased spatter on the base metal. The 0.016-in.-diameter electrode showed more repelled transfer at 80Ar-20CO_2 than the larger electrodes.

The appearance of repelled transfer is consistent with an increase in current density on the electrode and a subsequent increase in plasma pressure exerted on the droplet. The direction of the plasma pressure is upward and acts as an attaching force on the droplet. The droplet must then grow to a larger size in order to detach. In all cases, increasing the amounts of CO_2 above a critical level leads to plasma pressure becoming large enough to suspend the droplet and cause erratic detachment. Other researchers (Refs. 13, 14) have noted similar findings.

By using electrode diameters as thin as 0.016 in., the traditionally defined spray transfer mode was not achieved in CO_2 concentrations greater than 30%. It was expected that smaller electrode diameters would produce smaller droplet diameters and cause the arc to climb above the droplet forcing a transition from globular to spray, but this was not the case. Droplet diameters after the transition did not decrease proportionally with the decrease in electrode diameter, as shown schematically in Fig. 17. This is a key result of this research. Instead of droplet diameters becoming smaller with decreasing electrode diameters, the droplets remained relatively equal in size. The anode spot area is not significantly changed by the electrode diameter. The arc was unable to climb over the droplet, therefore no transition occurred. While operating, the process sounded and appeared to be spray transfer mode; however, detailed inspection of the laser shadowgraphs did not show the envelopment of the droplet by the arc, characteristic of spray transfer. Pulsing could potentially overcome this problem by detaching the droplets before they grow, and it is a current area of research.

Conclusions

This investigation extended the range of droplet detachment analysis in GMAW to electrodes as thin as 0.016 in. in binary Ar-CO_2 gas mixtures operated with DCEP. Voltage signal analysis and high-speed laser shadowgraphs were used to determine transfer mode, droplet detachment frequency, and average droplet diameters.

A newly designed contact tip was used with the 0.016-in. electrode that improved process stability. By precisely controlling the electrical contact point between the electrode and contact tip, the number of

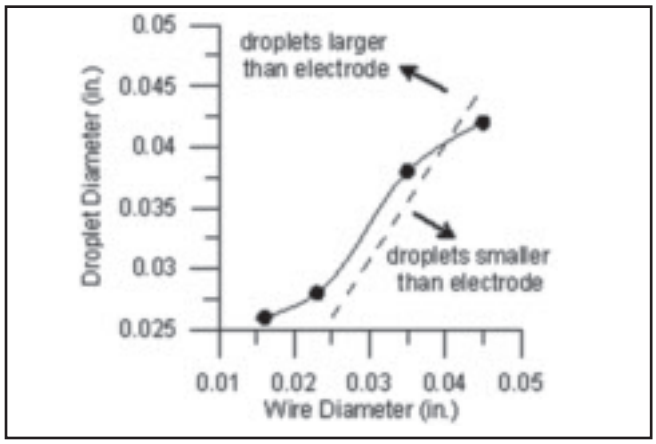

Fig. 15 — Droplet diameter in the spray region plotted against the electrode diameter.

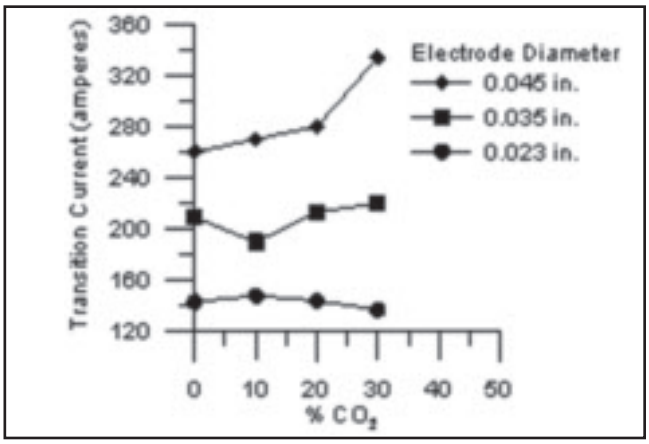

Fig. 16 — Transition currents for various electrode diameters in different composition shielding gases. The transition current here is defined as the average between the upper and lower shelves of droplet diameters. Above 30% CO_2, repelled transfer began to dominate. The 0.016-in.-diameter electrode is not included because the upper shelf was not found.

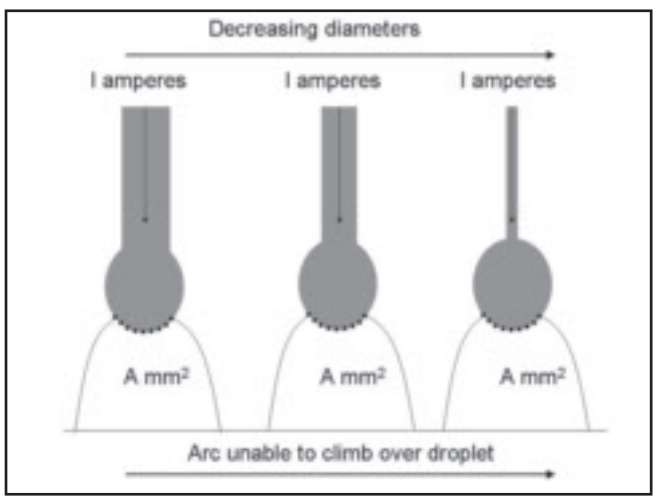

Fig. 17 — The arc is unable to climb up and envelop the droplet because droplet sizes do not decrease as electrode diameter decreases. Figure is not to scale.

meltback events decreased when compared to conventional tube-type designs.

Binary Ar-CO_2 shielding gas compositions were tested with CO_2 amounts up to 50%. At 30% CO_2, the process began to exhibit repelled transfer for the 0.045-, 0.035-, and 0.023-in. electrodes and at 20% CO_2 for the 0.016-in.-diameter electrode. During repelled transfer, the average droplet size grows larger than the electrode and observations from high-speed shadowgraphs suggest that the constricted arc might cause an upward force that levitates the droplet.

When operating in the stable metal transfer regime, a change in transfer mode with increasing current from large-diameter droplets at low detachment frequency to small-diameter droplets at high detachment frequency is seen in all electrode diameters when CO_2 concentrations in the shielding gas are lower than 30%. The average current used to define the transition is not much affected by the amount of CO_2 for small electrode diameters (0.023 and 0.035 in.) and increases slightly for 0.045 in. This supports previous findings as well as extends the results to the unexplored range of 0.016-in.-diameter electrodes.

The traditional classification of spray and globular transfer relies on comparing the diameter of the droplets to that of the electrode. However, the findings of this research indicate that this definition is not useful for 0.035-in. steel electrodes and smaller. All electrodes exhibited an increase in droplet detachment frequency with current as well as a transition from large- to small-diameter droplets. However, the average droplet size is still larger than the electrode diameter (up to about twice as large), regardless of current.

Acknowledgments

The authors would like to gratefully thank the American Welding Society Foundation for funding this research with a fellowship award. This work is also supported by the National Science Foundation CAREER award DMI-0547649. The authors also gratefully acknowledge the help of Bruce Albrecht from Miller Electric and Tom Siewert and Tim Quinn of the National Institute of Standards and Technology (NIST) in Boulder, Colo.

References

1. *Welding Handbook*, 7th ed., Vol. 1, Fundamentals of Welding. 1981. Ed. C. Weisman. Miami, Fla.: American Welding Society.

2. IIW, Classification of metal transfer. 1977. *Welding in the World* 15(5/6): 113–116.

3. Muller, A., Greene, W. J., and Rothschild, G. R. 1951. Characteristics of inert-gas-shielded metal arcs. *Welding Journal* 31(8): 717–727.

4. Lesnewich, A. 1958. Control of melting rate and metal transfer in gas-shielded metal-arc welding: Part I — Control of electrode melting rate. *Welding Journal* 37(8): 343-s to 353-s.

5. Lesnewich, A. 1958. Control of melting rate and metal transfer in gas-shielded metal-arc welding: Part II — Control of metal transfer. *Welding Journal* 37(9): 418-s to 425-s.

6. Rhee, S., and Kannatey-Asibu, E. 1991. Analysis of arc pressure effect on metal transfer in gas-metal arc-welding. *Journal of Applied Physics* 70(9): 5068–5075.

7. Wang, G., Huang, P. G., and Zhang, Y. M. 2003. Numerical analysis of metal transfer in gas metal arc welding. *Metallurgical and Materials Transactions B* 34B (June): 345–353.

8. Hu, J., and Tsai, H. L. 2006. Effects of current on droplet generation and arc plasma in gas metal arc welding. *Journal of Applied Physics*, 100 (Article No. 053304).

9. Rothschild, G. R. 1956. Carbon-dioxide-shielded consumable-electrode arc welding. *Welding Journal* 35(1): 19–29.

10. Smith, A. A. 1971. *CO_2 Welding of Steel*, 3rd ed. Cambridge, UK: The Welding Institute.

11. Rhee, S., and Kannatey-Asibu, E. 1992. Observation of metal transfer during gas metal arc welding. *Welding Journal* 71(11): 381–386.

12. Haidar, J., and Lowke, J. J. 1997. Effect of CO_2 shielding gas on metal droplet formation in arc welding. *IEEE Transactions on Plasma Science* 25(5): 931–936.

13. Mechev, V. S., et al. 1982. The thermal and physical-properties of gaseous carbon-dioxide and their effects on the welding arc. *Automatic Welding USSR* 35(4): 24–29.

14. Nemchinsky, V. A. 1996. The effect of the type of plasma gas on current constriction at the molten tip of an arc electrode. *J. Phys. D: Appl. Phys.* 29: 1202–1208.

15. Pires, I., Quintino, L., and Miranda, R. M. 2007. Analysis of the influence of shielding gas mixtures on the gas metal arc welding metal transfer modes and fume formation rate. *Materials & Design* 28(5): 1623–1631.

16. Lesnewich, A. 1955. Electrode activation for inert-gas-shielded metal-arc welding. *Welding Journal* 35(12): 1167–1178.

17. Cushman, E. 1961. Electrode for spatter-free welding of steel in carbon dioxide. *Welding Journal* 41(1): 14-s to 21-s.

18. Needham, J. C., and Carter, A. W. 1967. Arc and transfer characteristics of the steel/CO_2 welding process. *British Welding Journal* (10): 533–549.

19. Matsuda, F., Ushio, M., Nishikawa, H., and Yokoo, T. 1985. Pulsed GMAW — Spattering in pulsed CO_2 welding. *Transactions of JWRI* 14(1): 13–19.

20. Cuiuri, D., Norrish, J., and Cook, C. 2002. New approaches to controlling unstable gas metal arc welding. *Australasian Welding Journal* 47(3): 39–47.

21. Kim, Y. S., and Eagar, T. W. 1993. Analysis of metal transfer in gas metal arc-welding. *Welding Journal* 72(6): 269-s to 275-s.

22. Kohn, G., and Siewert, T. A. 1986. The effect of power supply response characteristics on droplet transfer of GMA welds. *Proceedings International Conference on Trends in Welding Research*. Gatlinburg, Tenn.: ASM International.

23. Liu, S., and Siewert, T. A. 1989. Metal transfer in gas metal arc welding droplet rate. *Welding Journal* 68(2): 52-s to 58-s.

24. Waszink, J. H., and Van Den Heuvel, G. J. P. M. 1982. Heat-generation and heat-flow in the filler metal in GMA welding. *Welding Journal* 61(8): 269-s to 282-s.

25. Mendez, P. F., and Soderstrom, E. 2005. Gas metal arc welding methods and apparatus, U.S. Patent Office application # 2006/0237411 A1, Editor.

26. Allemand, C. D., et al. 1985. A method of filming metal transfer in welding arcs. *Welding Journal* 64(1): 45–47.

CAN WE TALK?

The *Welding Journal* staff encourages an exchange of ideas with you, our readers. If you'd like to ask a question, share an idea or voice an opinion, you can call, write, e-mail or fax. Staff e-mail addresses are listed below, along with a guide to help you interact with the right person.

Publisher/Editor
Andrew Cullison
cullison@aws.org, Extension 249
Article Submissions

Senior Editor
Mary Ruth Johnsen
mjohnsen@aws.org, Extension 238
Feature Articles

Associate Editor
Howard Woodward
woodward@aws.org, Extension 244
Society News
Personnel

Assistant Editor
Kristin Campbell
kcampbell@aws.org, Extension 257
New Products
News of the Industry

Production Manager
Zaida Chavez
zaida@aws.org, Extension 265
Design and Production

Advertising Sales Director
Rob Saltzstein
salty@aws.org, Extension 243
Advertising Sales

Advertising Sales & Promotion Coordinator
Lea Garrigan Badwy
garrigan@aws.org, Extension 220
Production and Promotion

Advertising Production Manager
Frank Wilson
fwilson@aws.org, Extension 465
Advertising Production

Peer Review Coordinator
Erin Adams
eadams@aws.org, Extension 275
Peer Review of Research Papers

Welding Journal Dept.
550 N.W. LeJeune Rd.
Miami, FL 33126
(800) 443-9353
FAX (305) 443-7404

Acknowledgment

J. E. Ramirez, the author of the paper titled "Characterization of High-Strength Steel Weld Metals: Chemical Composition, Microstructure, and Nonmetallic Inclusions" published in the March 2008 issue of the *Welding Journal* (pages 65-s to 75-s), would like to report the omission of the following acknowledgment statement.

"The author would like to acknowledge the contribution of Dr. A. J. Ramirez, Mr. J. W. Sowards, and Dr. J. C. Lippold from The Ohio State University Welding & Joining Metallurgy Group, and Sue Fiore from EWI in the development of a database for microstructures of high-strength steel weld metals through an EWI-Cooperative Research Program (CRP). The author also would like to acknowledge all the member companies of EWI for funding the development of the database through the cooperative research program. The pictures associated with microstructures and nonmetallic inclusions in this publication are included in the developed database."